

Thermoeconomic approach for the analysis of control system of energy plants

*Original*

Thermoeconomic approach for the analysis of control system of energy plants / Verda, Vittorio; Baccino, Giorgia. - In: ENERGY. - ISSN 0360-5442. - 41:(2012), pp. 38-47. [10.1016/j.energy.2011.08.027]

*Availability:*

This version is available at: 11583/2501285 since:

*Publisher:*

Elsevier

*Published*

DOI:10.1016/j.energy.2011.08.027

*Terms of use:*

This article is made available under terms and conditions as specified in the corresponding bibliographic description in the repository

*Publisher copyright*

(Article begins on next page)

# Thermoeconomic Approach for the Analysis of Control System of Energy Plants

*Vittorio Verda\*, Giorgia Baccino*

*Energy Department - Polytechnic of Turin. C.so Duca degli Abruzzi 24. 10129 Turin. Italy.*

Energy, Volume 41, Issue 1, May 2012, Pages 38-47

## ABSTRACT

In this paper a thermoeconomic approach is applied to the dynamic model of a Power System in order to investigate the effects of the control system on the primary energy consumption and on the economic costs of the product. To achieve this objective, various control strategies are compared when variations of the operation condition, due to some internal or external causes, are produced.

These variations cause the intervention of the control system, which rearranges the operating condition in order to have the controlled quantities within acceptable ranges. Generally the plant efficiency changes, depending on the selected strategy. A microturbine is considered as the case study.

The analysis here proposed allows one to quantify the effect of the control on the performance variation of the components. The approach associates an exergetic cost and a thermoeconomic cost to the control system operation, which expresses the additional resource (primary energy and economic resources) consumptions that may be associated to the control. The impact on the initial and final steady states as well as the transient evolution are considered. This can be usefully applied to improve energy system operation acting on the control system, both in the off-design steady states and transient operations. In the particular application considered in this paper, reductions of about 8% in fuel consumption and 5% in the total costs

---

\* Corresponding author

are achieved. Concerning transient operation, it is shown that the control system can produce large variation in the operation costs.

Keywords: Thermoeconomic analysis; Control system analysis; Control improvement

## NOMENCLATURE

$A^t$	Total internal exergy [kJ];
$b$	Specific exergy [kJ/kg];
$c$	Unit cost [€/kJ];
$C$	Total investment cost [€];
$C$	Torque [N·m]
$c_p$	Specific heat [kJ/kgK];
$E_{ij}$	Flow of the productive structure [kW];
$E_c$	Kinetic energy [kJ];
$E_p$	Potential energy [kJ];
$h$	Specific enthalpy [kJ/kg];
$h$	Operating hours per year;
$i$	Interest rate;
$k_{ij}$	Unit exergy consumption [kW/kW];
$k^*$	Exergetic unit cost of a flow [kW/kW];
$J$	Inertia [kg·m <sup>2</sup> ];
$m$	Mass flow rate [kg/s];
$n$	Number of years;
$N$	Rotational speed [r/min];
$p$	Pressure [bar];
$P_i$	Product of the $i^{\text{th}}$ component [kW];
$R$	Specific gas constant [kJ/kgK];
$R$	Radius [m];

S	Entropy [kJ/K]
s	Specific entropy [kJ/kgK];
t	time [s];
T	Temperature [°C];
U	Internal energy [kJ];
W	Power [kW];
Z	Total investment cost rate [€/s];
$\Delta F_T$	Total fuel impact [kW];
$\Psi$	Exergy flow [kW];
$\Psi^*$	Exergetic cost of a flow [kW];
$\omega$	Angular rotational velocity [rad/s];
$\rho$	Density [kg/m <sup>3</sup> ];
$\sigma$	Stress [N/m <sup>2</sup> ];

### Subscripts

0	Ambient condition;
a	air;
c	fuel;
cv	control volume
F	resource;
FT	external resource (fuel);
g	combustion gas;
P	product;
w	water.

## INTRODUCTION

The control system of a power plant attain the set point of some variables and restore them as fast as possible when some deviations occur through actions on control devices. A proper control can obtain more production out of limited plant equipment and can contribute to reducing operating costs more than any other device; however, also a control technology entails costs that cannot be neglected [1].

The control system must be taken into account whatever is the aim of the analysis: cost accounting, performance/cost evaluation [2], operation and management optimization [3], detection and location of malfunctions [4], etc. In this paper, the analysis of the control system is performed using thermoeconomics.

Thermoeconomic methodologies have been widely applied to the analysis of energy systems. Some of the possible goals are cost accounting, system improvements, and diagnosis [5, 6]. The reason for using this methodology in the analysis of control strategies is that thermoeconomics allows one to calculate the additional fuel consumption and the additional economic costs that can be ascribed to the control system.

The word “additional” means that two operating conditions should be compared. These two conditions are the operating condition corresponding with the control strategy to evaluate and a reference condition, which may be the nominal operating condition. The calculation of the additional fuel consumption cannot be always obtained through simple comparison of the fuel consumption in two conditions, because the plant load in the two conditions may be different. In the case of a multi-product systems this is even more evident, as one of the products may be the same in the two conditions, but the other products are generally different. A tool called the “fuel impact formula” has been developed within thermoeconomic diagnosis [7, 8]. This tool allows one to calculate, in any operating condition, the additional fuel consumption with respect to a reference condition.

Two terms contribute to the fuel impact: the variations in the efficiency of components due to off-design conditions or intrinsic malfunctions and the variations in the overall plant production:

$$\Delta F_T = \sum_{i=1}^n \left( \sum_{j=0}^n k_{p_j}^* \cdot \Delta k_{ji} \right) \cdot P_i^0 + \sum_{i=1}^n k_{p_i}^* \cdot \Delta P_{e_i} \quad (1)$$

$k_{p_j}^*$  is the exergetic unit cost of the product of the  $j^{\text{th}}$  component (calculated in operating condition),  $P_j^0$  is the total product of  $i^{\text{th}}$  component in reference condition and  $k_{ji}$  is the unit exergy consumption defined as:

$$k_{ji} = \frac{E_{ji}}{P_i} \quad (2)$$

where  $E_{ji}$  is the resource of the  $i^{\text{th}}$  component produced by the  $j^{\text{th}}$  component ( $0^{\text{th}}$  component is the ambient).  $\Delta k_{ji}$  is the variation of  $k_{ji}$  between the operating condition and the reference condition. The term  $\Delta P_{ei}$  is the variation between the overall system product generated by the  $i^{\text{th}}$  component in the operating condition and that in the reference condition.

The first term on the right hand side of equation (1) expresses the additional fuel consumption required to obtain the same overall production as in the reference condition. This quantity can be used to evaluate the impact of the system together with its control in a particular steady state operating condition. When comparing alternative control strategies, the differences in its value can be directly associated to inefficiencies caused by the control system. Similar approach can be used for the analysis of the economic impact. Thermoeconomics is usually formulated considering steady state conditions. This is not suitable to evaluate control strategies and a theoretical development is necessary.

In a previous paper [9], thermoeconomic analysis was used to compare various control strategies for a gas turbine and to define the cost of a control system. The analysis was conducted considering the initial and final steady states, without including the impact of the control system on the transient process and the deviation with respect to the desired operating condition. In a recent paper [10], some preliminary work has been presented also considering transient behavior. In particular, the exergetic cost analysis was conducted considering two control strategies for a microturbine. Nevertheless, the analysis has highlighted the need for a complete thermoeconomic approach. Here, the tool for such analysis is presented and applied to the same microturbine. The comparison between the exergetic cost analysis and thermoeconomic analysis is also performed.

## **THERMOECONOMIC ANALYSIS IN TRANSIENT CONDITIONS**

Thermoeconomic analysis of control system operation should include the transient operation from the initial operating condition to the final operating condition. Such analysis requires to consider the contribution of exergy storage to calculate both the exergetic and economic unit costs.

To analyze this contribution, we may start from the general exergy equation for a control volume:

$$\sum_{i=1}^m \Psi_{q_i} - W_t = \sum_{j=1}^n m_j \cdot b_j^t + \Psi_{irr} + \left( \frac{\partial A^t}{\partial t} \right)_{cv} \quad (3)$$

where  $\Psi_q$  is the exergy associated with heat fluxes exchanged between the component and other systems,  $W_t$  is the mechanical work,  $m$  is the general mass flow rate exiting (+) or entering (-) the system and  $b$  the corresponding total specific exergy,  $\Psi_{irr}$  accounts for the irreversibilities,  $A^t$  is the total internal exergy in the control volume (cv):

$$A^t = U + p_0 \cdot V - T_0 \cdot S + E_c + E_p \quad (4)$$

where  $U$  is the internal energy,  $p_0$  is the biosphere pressure,  $V$  the system volume,  $T_0$  the biosphere temperature,  $S$  the system entropy,  $E_c$  the kinetic energy and  $E_p$  the potential energy. Internal exergy can be written either with or without reference state (i.e.  $A^t - A_0^t$ ) as the latter is constant, thus its time derivative is zero.

The same equation can be rewritten in terms of entering and exiting exergy flows and fluxes or, which is the choice operated here, productive flows. This is obtained by rearranging the physical flows in order to define resources (F), products (P) and losses (L) for the various control volumes. The product expresses the goal of a component, i.e. the useful result of the process occurring in the component. The product can be used by other components of the system or made available to the ambient (overall system product). The resource is the ensemble of exergy required by the component to develop its productive process. The resource can be either made available from the ambient or by other components of the system. The loss is a possible amount of exergy associated to a physical flow exiting the plant and lost without being used. Productive flows may be in the form of thermal exergy, mechanical exergy or exergy associated to mass flows. The exergy equation in terms of productive flows is written:

$$\Psi_F = \Psi_P + \Psi_L + \left( \frac{\partial A^t}{\partial t} \right)_{cv} + \Psi_{irr} \quad (5)$$

Equation (5) shows that, in a general process, the exergy flow entering with the resources is converted into products, dissipated in losses, stored or destroyed as irreversibilities.

The corresponding exergetic cost balance is:

$$\Psi_F^* = \Psi_P^* + \left( \frac{\partial A^t}{\partial t} \right)_{cv}^* \quad (6)$$

where  $\Psi_i^*$  is the exergetic cost associated to the exergy flow  $\Psi_i$ , i.e. the exergy of natural resources required to generate that flow [5].

To calculate the exergetic costs, the unit cost of exergy stored in a control volume is assumed equal to the exergetic unit cost of the products of that component, namely:

$$\Psi_F \cdot k_F^* = \left( \Psi_P + \left( \frac{\partial A^t}{\partial t} \right)_{cv} \right) \cdot k_P^* \quad (7)$$

where  $k^*$  are the exergetic unit costs. A zero cost for losses and irreversibilities causes an increase in the exergetic unit cost of the component product P with respect to its resource F, as  $\Psi_P + \left( \frac{\partial A^t}{\partial t} \right)_{cv} \leq \Psi_F$ .

Similar approach can be used to calculate economic unit costs. The balance equation is:

$$\Psi_F \cdot c_F + Z = \left( \Psi_P + \left( \frac{\partial A^t}{\partial t} \right)_{cv} \right) \cdot c_P \quad (8)$$

where  $c$  are the economic unit costs and  $Z$  is the cost rate of the component. This last term makes the difference with respect to equation 7 as it allows one to account for the effects of the control strategy on the component lifetime. Cost rate is calculated as:

$$Z = \frac{C}{3600 \cdot h} \cdot \frac{i \cdot (1+i)^n}{(1+i)^n - 1} \quad (9)$$

where  $C$  is the total investment cost of the component,  $h$  the operating hours per year,  $i$  the interest rate and  $n$  the lifetime (in years). A control strategy may have a positive effect on the efficiency and thus cause a negative additional fuel consumption. Nevertheless, the control strategy may have a negative effect on the component lifetime. Thermoeconomic analysis allows one to compare these two effects. In control system analysis, the total additional cost rate can be calculated. This quantity is defined as the cost rate due to the additional fuel consumption plus the difference between the current investment cost rate (i.e. considering the current lifetime) and the reference investment cost rate (i.e. evaluated considering the reference lifetime), namely:



$$\Delta\Pi = \Delta F_T \cdot c_{FT} + (Z - Z_{ref}) \quad (10)$$

where  $c_{FT}$  is the economic unit cost of the fuel, i.e. the overall system resource entering the plant from the environment.

## ANALYSIS OF A MICROTURBINE

A cogenerative microturbine is considered as an application. A zero-dimension physical model of this system has been built using the software EES. All the components have been considered in steady state, except for the block compressor+turbine+shaft, whose inertia has been considered. The model considers energy, mass and momentum conservation for all the components, proper constitutive equations for the physical phenomena (e.g. heat transfer in the heat exchangers, non-isentropic compression and expansion, etc.), performance curves for the off-design operation of components (e.g. effectiveness-NTU for the heat exchangers, performance maps for compressor and turbine [11]) and fluid properties. The model also includes cost equations of the various components as well as cost balances and additional equations for the calculation of the unit costs. Additional details are available in the Annex.

This model (indicated as “model 1” hereafter) does not include the control laws. These are considered in a second model (model 2), built in the environment Matlab-Simulink. A schematic of model 2 is presented in Figure 1. Some of the blocks model the physical behavior of the components, while the other blocks model the control system.

The Microturbine block synthesizes compressor and turbine behavior, using a quadratic regression function to link the net torque (output variable) to the external air temperature, fuel mass flow rate and rotational speed of the shaft (input variables). This function has been obtained using the steady state model (model 1) of the turbine:

$$C_{net} = c_1 + c_2 X_1 + c_3 X_2 + c_4 X_3 + c_5 X_1 X_2 + c_6 X_1 X_3 + c_7 X_2 X_3 + c_8 X_1^2 + c_9 X_2^2 + c_{10} X_3^2 \quad (11)$$

where  $C_{net}$  is the net torque (i.e. the difference between the turbine torque and the compressor torque), the  $c_i$  are regression coefficients ( $c_1=5.63 \text{ N}\cdot\text{m}$ ;  $c_2=27.89 \text{ N}\cdot\text{m}$ ;  $c_3=-15.11 \text{ N}\cdot\text{m}$ ;  $c_4=5.92 \text{ N}\cdot\text{m}$ ;  $c_5=-98.13 \text{ N}\cdot\text{m}$ ;  $c_6=58.81 \text{ N}\cdot\text{m}$ ;  $c_7=-148.52 \text{ N}\cdot\text{m}$ ;  $c_8=22.19 \text{ N}\cdot\text{m}$ ;  $c_9=116.56 \text{ N}\cdot\text{m}$ ;  $c_{10}=39.83 \text{ N}\cdot\text{m}$ ),  $X_1$  is the ratio between the

current speed and the nominal shaft speed,  $X_2$  is the ratio between the fuel mass flow rate and its nominal value,  $X_3$  is the ratio between the external air temperature and the nominal temperature. A comparison between 300 values, corresponding with different values of the input parameters (free operation parameters) calculated using model 1 in steady state and those obtained with equation (11) is shown in Figure 2.

The Generator block calculates the resistance torque ( $C_r$ ) as the ratio between the requested mechanical power (obtained from the electric power and the electrical efficiency of the inverter) and the current rotational speed. The net torque (turbine torque minus the compressor torque) and the generator torque complies the mechanical balance:

$$C_{net} = C_r + J \frac{d\omega}{dt} \quad (12)$$

where  $J$  is the total moment of inertia (shaft, compressor and turbine) and  $\omega$  is the angular rotational speed of the shaft. The integrator allows one to obtain the current rotational speed. A saturation block positioned on generator speed input limits possible speed peaks to maximum speed value. This may occur in the case of brusque drop of the generator torque.

The last physical block is that named TOT. This block calculates the turbine outlet temperature (TOT) as a quadratic function of the external temperature, the electric power and the rotational speed. As in the case of the net torque, the results of this model are compared with those obtained from the physical model.

As for the control strategies, their goal is the obtainment of the desired electric power keeping the operating temperatures within proper limits in order to avoid too low efficiencies or low lifetime due to creep. A first strategy here examined is operated considering the turbine outlet temperature as constant. This is a typical operating mode for microturbines [12].

The upper part of Figure 1 contains the temperature control. The turbine outlet temperature is compared with the reference value. In the case there is a difference, the control system operates on the fuel mass flow rate. The block on the upper right corner is a function calculating the optimal fuel mass flow rate depending on the requested electric load. This is a reference value and the control system may correct the final value if the TOT differs from the set point (in the case of the first control strategy). This difference also corrects the resistance torque felt by the system, which allows one to modify the rotational velocity. A proportional integrative (PI) control has been selected. The selected values of the proportional and integrative constants

are  $4 \cdot 10^{-6}$  and  $1 \cdot 10^{-5}$ , respectively. Both values are assumed as the result of an optimization procedure, which is discussed in the following. The discussion is limited to the values assumed by the first parameter, as the second one does not affect significantly the results. The control strategy is evaluated considering a step increase in the requested electric power from 75 kW to 110 kW.

Figure 3 shows a comparison between electricity request and the actual electric power. In the initial condition, the electric load is about 1.7 kW smaller than the request. When the request is increased, the electricity production increases as well, with an increasing deviation in the ramp, up to 2.5 kW. This deviation still increases to about 2.7 kW as the system proceed to final steady state. Thermal exergy flux produced by the system increases from about 32.5 kW to about 35.3 kW, as is also shown in Figure 3.

The control strategy in this case operates an increase in the rotational speed when the requested load increases. The corresponding inertial term registers a non negligible peak, which is also shown in Figure 3.

Figure 4 shows the total fuel impact corresponding with the use of the presented control strategy. In the initial operating condition, the fuel impact due to inefficiencies is about 15 kW. When the electricity request increases, the fuel impact decreases, to reach the steady state value of about -4 kW. In order to explain this behavior, the contributions of the various components to the fuel impact are shown in Figure 5 in the initial and the final operating condition. Each of these contributions is a term of the summation on the right hand side of equation 1. These are obtained by considering the operation at nominal load as the reference condition, thus the  $\Delta k_{ji}$ s are the differences between unit exergy consumptions in the actual operating condition (initial steady state and final steady state) and that calculated at nominal load. Calculations have been performed by considering the productive structure presented in the Annex.

The effect that mostly contributes to the reduction in the total fuel impact is the different operation of the combustion chamber. This is caused by the smaller value in the turbine inlet temperature at partial electric load, as shown in Figure 6.

It is now interesting to show the effects on the fuel impact that are produced by modifying the value of the proportional constant in the control law. This result is shown in Figure 7. Starting from the selected value of the proportional constant, which is marked in the figure, an increase produces a small decrease in the fuel impact and then a small increase. In contrast, when the value is reduced, the fuel impact increases up to about 22 kW and then decreases to about 12 kW, which is smaller than the impact in the case of the

selected value of the constant. The reason to chose  $k_p=6 \cdot 10^{-6}$  instead of  $1 \cdot 10^{-7}$  is related to the economic impact. This evaluation requires to consider the effect of turbine temperature on the lifetime.

When turbine materials are subjected to stress and operate at high temperature, they suffer from plastic deformation, known as creep. Engine manufacturers normally quote engine life when the engine is operating at 100% power at ISO conditions. In particular, in this case, this time corresponds to more than 60000 hours; however, a microturbine rarely operates at ISO ratings.

Different control strategies aim at obtaining a system able to satisfy quite immediately a request power, even though that means, sometimes, going through temperatures that may reduce its longevity. It is important to evaluate the system lifetime, and relative costs, in different operative conditions imposed by the use of different types of control. For the calculation, it is hypothesized that the microturbine operates in the field of the so called secondary creep. It has been also hypothesized that blades material is a Nickel alloy characterized by a density of about 8000 kg/m<sup>3</sup>. The maximum stress value has been calculated assuming a shaft angular velocity of 7330 rad/s, a 95 mm internal diameter and a 70 mm external diameter as:

$$\sigma_{\max} = \frac{\rho \cdot \omega^2}{2} \cdot (R_e^2 - R_i^2) \quad (13)$$

where  $\rho$  is the material density,  $\omega$  is the angular velocity,  $R_e$  and  $R_i$  the external and internal radius. To correlate rupture stress value ( $\sigma$ ), operating temperature ( $T$ ) and rupture time ( $t_R$ ), the Larson Miller Parameter has been used [13]. This parameter aims to build a unique curve on the plane ( $f(T)$ ,  $\log(t_R)$ ) starting from an aggregate of stress – deformation curves, assuming  $\sigma$  as parameter. For the examined microturbine, the Larson Miller parameter corresponding to nominal condition is calculated as:

$$P_{LM} = T(C + \log_{10} t_R) \quad (14)$$

where  $P_{LM}$  is the Larson Miller Parameter,  $C$  is a coefficient (equal to 20),  $t_R$  is the rupture time assumed equal to 60000 hours, and  $T$  is an average value between the nominal turbine inlet temperature and the nominal turbine outlet temperature obtained from CFD analysis of the turbine. Temperature distribution in the turbine in nominal condition is shown in Figure 9.

A graph ( $P_{LM}$ ,  $\log(\sigma)$ ) has been built considering nickel alloy data and typical microturbine operating parameters. This curve is shown in Figure 10.

For different operating conditions, and in particular for different temperature values obtained for the control technologies modelled, the corresponding time rupture has been calculated as:

$$t_R = 10^{\frac{P_{LM} - C}{T}} \quad (15)$$

Once the lifetime is calculated, the additional cost expressed by equation (10) can be calculated. This is shown in Figure 11 (plain line). Additional cost rate is about  $2.5 \cdot 10^{-4}$  €/s in the initial operating condition. This cost is mainly due to the inefficiencies at partial load and is about 5% of the total cost rate in this condition. In the transient operation, this cost decreases and becomes very close to the final value ( $4.5 \cdot 10^{-5}$  €/s) after about 400 s from the load variation. If the proportional constant is increased, the shape of this curve remains almost unvaried, but the cost decrease becomes slower. If the constant is reduced with respect to the selected value, the cost decrease becomes quicker. The additional cost rate for  $k_p = 5 \cdot 10^{-6}$  is shown in the figure (dashed line). If this constant is reduced below  $3 \cdot 10^{-6}$  the shape of the additional cost rate changes and a peak appears. This is due to the high temperatures registered during the transient operation, which causes a reduction in the lifetime of the turbine. The additional cost rate for  $k_p = 1 \cdot 10^{-6}$  is shown in the figure (dotted line). The three curves in figure 11 shows that the constant value only modified the additional cost in the transient operation. To summarize the effect of proportional constant, Figure 12 shows the additional cost rate in the transient phase (plain line) and in the complete operation from  $t=0$ s to  $t=1200$ s (dotted line) as the function of the constant value.

The selected value of the proportional constant is thus a compromise between the fuel impact value in the initial operating condition and the additional cost in the transient operation.

An improvement with respect to this control strategy can be achieved by using a different control scheme. This permits to decouple the operations on the fuel mass flow rate and on the rotational speed. A possible scheme is shown in Figure 13. The main difference with respect to the previous scheme is the block in blue. This part allows the system to artificially increase the resistant torque when the calculated inlet turbine temperature is below the set value, so that the shaft decelerate and a lower air mass flow rate flows through the compressor, which causes an increase in the combustion temperature.

Using this scheme, the additional costs become those shown in Figure 14. Costs are reduced in the initial steady state and in the transient operation.

Further analysis can be conducted by splitting the two contributions to the additional costs: the contribution associated with the additional fuel consumption and that with the additional investment cost. These contributions are presented in figure 15.

In the initial operating condition, the contribution due to the investment cost is positive. This is due to the inlet turbine temperature, larger than the design value. In this condition the contribution due to the fuel impact is negative because of the larger efficiency. As the absolute value of this second contribution is smaller than the first one, the total cost can be further reduced by modifying the control strategy so that the turbine temperature corresponding with the initial condition is reduced.

In the transient operation and the final steady state the additional costs are negative and close to the nominal condition, which means that the control strategy does not need to be further modified in this part.

## **CONCLUSIONS**

Control systems are usually analyzed on the basis of their stability and robustness. In this paper, thermoeconomic analysis is used to evaluate, compare and improve control strategies for an energy system, considering their effects on primary energy consumption.

The additional fuel consumption and the additional economic cost, written for a transient system are used for this goal. These tools can be used both as indicators to evaluate the control performance and as a way to improve the control strategy. The application to the control law of a microturbine is proposed. It is shown that fuel consumption and operational cost at part load operation can be significantly reduced with respect to the values that can be achieved with control strategies typically used for these devices (i.e. constant value of the outlet turbine temperature). In addition, proper selection of the control law parameters allows one to reduce costs in transient operation.

## **ANNEX**

The microturbine is a power generation system that is based on a combination of a small gas turbine and a directly driven high-speed generator. A schematic of the plant considered in the present analysis is presented in figure A1.

The basic components of the microturbine system modelled are the compressor, the recuperator (air pre-heater), the combustion chamber and the turbine generator.

The heart of the microturbine is the compressor – turbine package, which is commonly mounted on a single shaft along with the electric generator.

Recuperators are heat exchangers that use the turbine hot exhaust gas to preheat the compressed air going into the combustor, thereby reducing the fuel needed to heat the compressed air to turbine inlet temperature.

The generator is placed on the same shaft as the compressor and the turbine.

The electricity created by the high-speed generator is converted into AC voltage with a constant frequency by a power converter that is a part of the power electronics. The power electronics control the electric variables of the microturbine and the machine can readily be connected to the power grid.

Only compressor – turbine package, recuperator and combustion chamber have been modelled; electric generator equations are been neglected, and so friction.

The model is built in Engineering Equation Solver (EES). System components modelled are compressor, air pre-heater, combustion chamber, gas turbine and heat exchanger.

Inlet air temperature, induction pressure and rotation speed (number of revolutions) have been assigned; in design conditions the air compressor is characterized by a pressure ratio of 4.9 and an isentropic efficiency of 0.8. Delivery temperature has been calculated assuming the transformation as adiabatic.

Off design conditions are modelled through proper characteristic maps; the compressor maps express pressure ratio ( $\beta_c = p_2/p_1$ ) and isentropic efficiency as the function of the non-dimensional mass flow rate

(corrected air mass flow rate,  $\frac{m_a \cdot \sqrt{T}}{p}$ ) and the non-dimensional speed (corrected shaft rotation speed,

$\frac{N_c}{\sqrt{T}}$ ). These have been obtained from [14].

Heat exchangers (air pre-heater and exhaust gas – water heat exchanger) are modelled using the  $\epsilon$ -NTU method. This consists of the energy equation applied to hot and cold fluids as well as a set of equations

depending on the heat exchange configuration. These equations relate one of the outlet temperatures to the inlet temperatures, the two heat capacities, the heat transfer area and the overall heat transfer coefficient. This approach can be used both for the design conditions and the off-design conditions.

The product of exchange area and heat transfer coefficient (UA) has been set to 4.13.

The combustion chamber is modeled with energy conservation equations. The microturbine burns natural gas, with a lower heating value of 47432 kJ/kg. The burner has an efficiency of 0.98.

In nominal conditions, the fuel mass flow rate is 0.007667 kg/s, but in off-design conditions it changes according to energy balance wrote for system component and on the basis of the off design value of air and gas mass flow rates.

The turbine is installed on the same shaft as the compressor, producing enough torque to power the compressor and the generator. In design conditions the microturbine isentropic efficiency is equal to 0.84 and the pressure ratio about to 4.6; off-design conditions of the microturbine are modelled through proper characteristic maps. Similarly as the compressor, turbine maps express the pressure ratio ( $\beta_t = p_4/p_5$ ) and

the turbine isentropic efficiency as function of corrected mass flow  $\frac{m_g \cdot \sqrt{T}}{p}$  and the corrected speed  $\frac{N_t}{\sqrt{T}}$  [14].

The end point of the system is a heat exchanger that interfaces exhaust gases and use water. Inlet and outlet water temperature is fixed respectively to a value of 333 K and 353 K , whereas it has been assumed that water flow rate can vary. As for the air pre – heater, heat exchanger has been modelled using  $\epsilon$ -NTU method. The product of exchange area and heat transfer coefficient (UA) has been set to 3.32.

The model has been validated considering data corresponding to steady-state operating conditions available in the literature [15].

The heart of thermoeconomic analysis is represented by the productive structure of the power plant, which is the mathematical expression of the role played by every component in the system. This description leans on the concepts of fuel and product. In modern thermoeconomics fuels and products are expressed as exergy flows. A general representation of the productive structure can be obtained by using the structural theory. A possible productive structure corresponding to the analyzed plant is represented in figure A2.



The compressor has one resource, the mechanical power supplied by the turbine ( $E_{41}$ ) and four products: mechanical and thermal exergy supplied to the air pre-heater ( $E_{12}$ ) and mechanical exergy supplied to the combustion chamber ( $E_{13}$ ), to the turbine ( $E_{14}$ ) and to the heat exchanger ( $E_{15}$ ).

The air pre-heater uses thermal exergy, that is considered as produced by the combustion chamber ( $E_{32}$ ) and mechanical exergy (associated with pressure losses) to increase the thermal exergy of the air flow ( $E_{23}$ ). The combustor (CC) has three resources: the total exergy flow of the fuel ( $E_{03}$ ), the mechanical exergy supplied by the compressor and the thermal exergy supplied by the air pre-heater and produces thermal exergy to feed the other components.

The turbine produces mechanical power, which is supplied to the air compressor and to the generator, which produces electricity ( $E_{60}$ ).

The heat exchanger uses mechanical and thermal exergy to increase the thermal exergy of a water flow, supplied to the users ( $E_{50}$ ).

$$E_{03} = m_f \cdot H_i \quad (A1)$$

$$E_{12} = m_a \left[ c_{pa} \left( T_1 - T_0 - T_0 \ln \frac{T_1}{T_0} \right) + R \cdot T_0 \cdot \ln \frac{p_1}{p_2} \right] + m_g \cdot R \cdot T_0 \cdot \ln \frac{p_5}{p_6} \quad (A2)$$

$$E_{13} = m_a \cdot R \cdot T_0 \cdot \ln \frac{p_2}{p_4} \quad (A3)$$

$$E_{14} = m_a \cdot R \cdot T_0 \cdot \ln \frac{p_4}{p_5} \quad (A4)$$

$$E_{15} = m_a \cdot R \cdot T_0 \cdot \ln \frac{p_6}{p_0} \quad (A5)$$

$$E_{23} = m_a \cdot c_p \left( T_2 - T_1 - T_0 \ln \frac{T_2}{T_1} \right) \quad (A6)$$

$$E_{32} = m_g \cdot c_{pg} \left( T_5 - T_6 - T_0 \ln \frac{T_5}{T_6} \right) \quad (A7)$$

$$E_{34} = m_g \cdot c_{pg} \left( T_4 - T_5 - T_0 \ln \frac{T_4}{T_5} \right) \quad (A8)$$

$$E_{35} = m_g \cdot c_{pg} \left( T_6 - T_7 - T_0 \ln \frac{T_6}{T_7} \right) \quad (A9)$$

$$E_{41} = W_8 \quad (A10)$$

$$E_{46} = W_9 \quad (A11)$$

$$E_{50} = m_w \cdot c_w \left( T_{12} - T_{11} - T_0 \ln \frac{T_{12}}{T_{11}} \right) \quad (A12)$$

$$E_{60} = W_{10} \quad (A13)$$

## References

- [1] F.G. Shinskey (1978). Energy Conservation through control. Academic Press. New York.
- [2] Y.M. El-Sayed (1999). Thermoeconomics of some options of large mechanical vapor-compression units. Desalination 125: 251-257.
- [3] D.F. Rancruel, M. R. von Spakovsky (2006). Decomposition with thermoeconomic isolation applied to the optimal synthesis/design and operation of an advanced tactical aircraft system. Energy 31: 3327–3341
- [4] V. Verda, L. Serra, A. Valero (2004). The effects of the control system on the thermoeconomic diagnosis of a power plant. Energy 29: 331-359
- [5] Lozano MA, Valero A. Theory of the Exergetic Cost. Energy 1993; 18 (9): 939-960.
- [6] Bejan A, Tsatsaronis G, Moran M. Thermal Design and Optimization. New York: John Wiley and Sons, 1996
- [7] Lozano MA, Bartolomé JL, Valero A, Reini M. Thermoeconomic Diagnosis of Energy Systems. In: Carnevale E, Manfrida G, Martelli F. Flowers 94. Florence World Energy Research Symposium. Padova: Sge, 1994. 149-156.
- [8] Reini M., Taccani R. (2002). On Energy Diagnosis of Steam Power Plants: a Comparison among three Global Losses Formulation. International Journal of Applied Thermodynamics.5: 177-188.

- [9] V. Verda, R. Borchellini (2004). Exergetic and economic evaluation of control strategies for a gas turbine plant. *Energy* 29:2253-2271
- [10] G. Baccino, M. Dalla Vedova, V. Verda (2010). Thermoeconomic Analysis of Energy System Control Strategies. *Proceedings of ECOS 2010*. Lausanne, Switzerland. June 14-17.
- [11] S. Haugwitz (2002). *Modelling of Microturbine Systems*. Master Thesis. Lund Institute of Technology.
- [12] M. Badami, A. Portoraro, G. Ruscica (2009). Analysis and Comparison of Performance of Two Small-Scale Trigeneration Plants: An ICE With a Liquid Desiccant Cooling System and a MGT With an Absorption Chiller. *Proceedings of ASME 2009 International Mechanical Engineering Congress and Exposition (IMECE2009)*. Lake Buena Vista, Florida. November 13–19.
- [13] Larson F. R., Miller J. (1952). A Time-Temperature Relationship for Rupture and Creep Stress *Transactions of the ASME*, 74, ASME, New York, July: 785-771
- [14] W. Wang, R. Cai, N. Zhang (2004). General characteristics of single shaft microturbine set at variable speed operation and its optimization. *Applied Thermal Engineering* 24: 1851–1863
- [15] C. Hin, J. Bailey, J.S. Wallace (2010). Heat Recovery from a Microturbine System. *Proceedings of the ASME conference on Energy Sustainability*. Phoenix, Arizona. May 17-22.

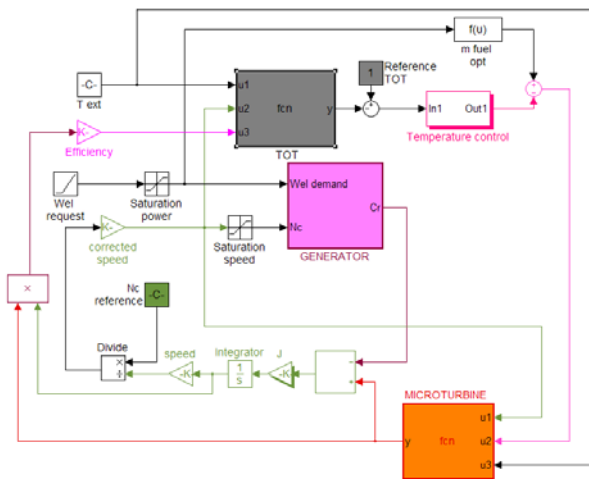


Figure 1. Schematic of the first control model

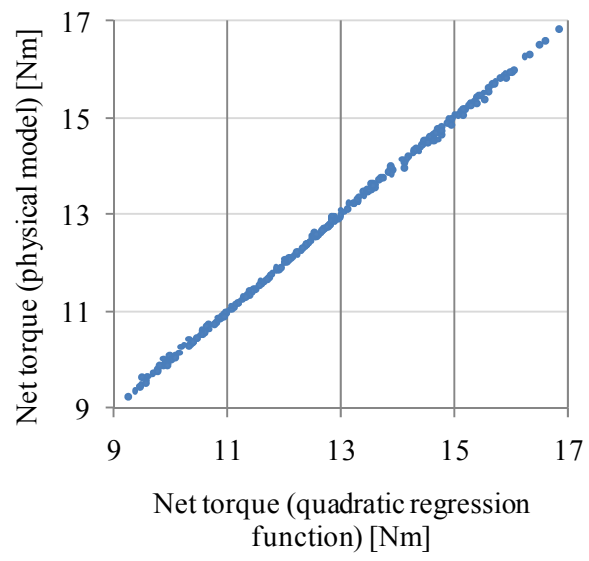


Figure 2. Comparison between the net torque calculated with the physical model and with equation (7)

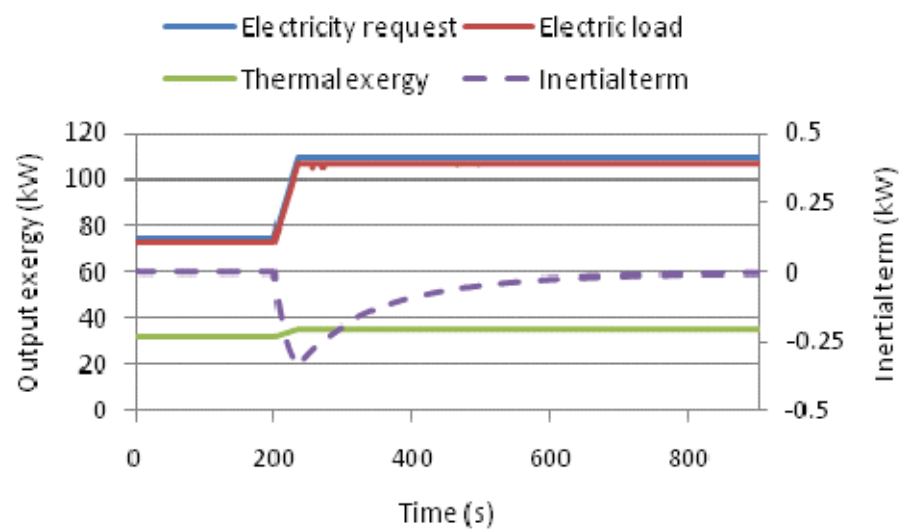


Figure 3. Exergy fluxes produced by the first system configuration

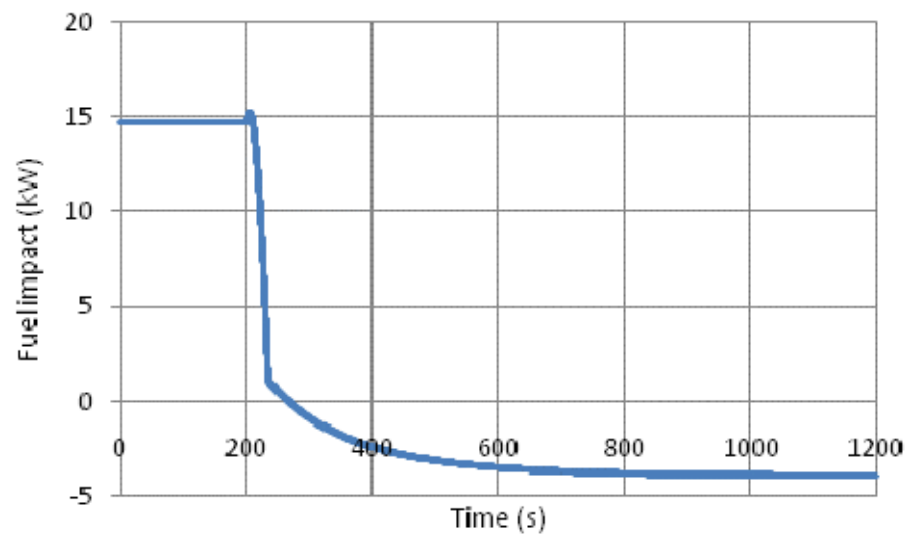


Figure 4. Fuel impact corresponding with the first control strategy

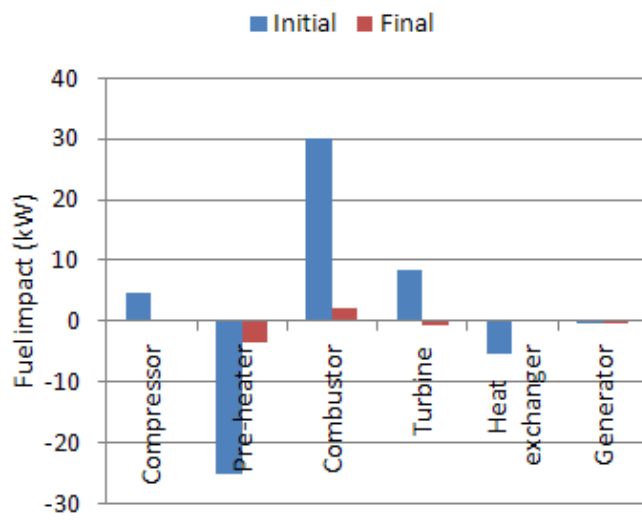


Figure 5. Fuel impact in the various components



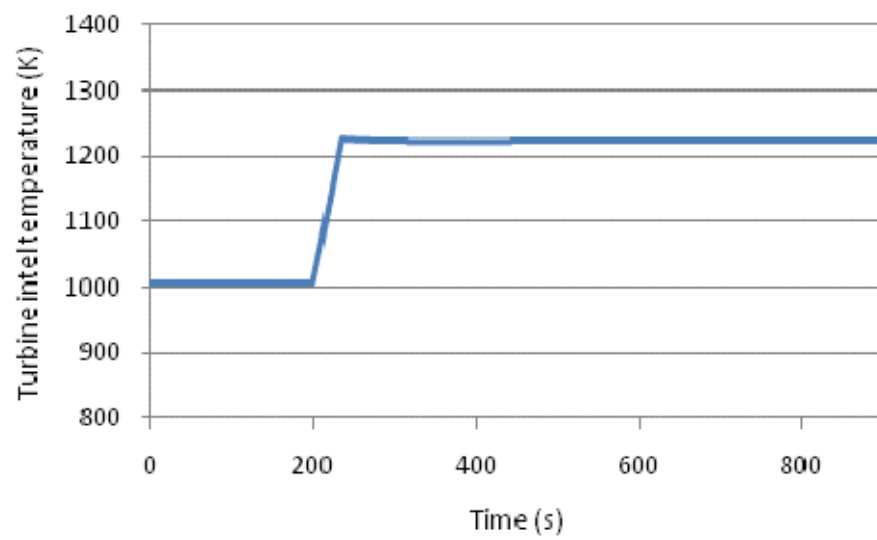


Figure 6. Evolution of the inlet turbine temperature

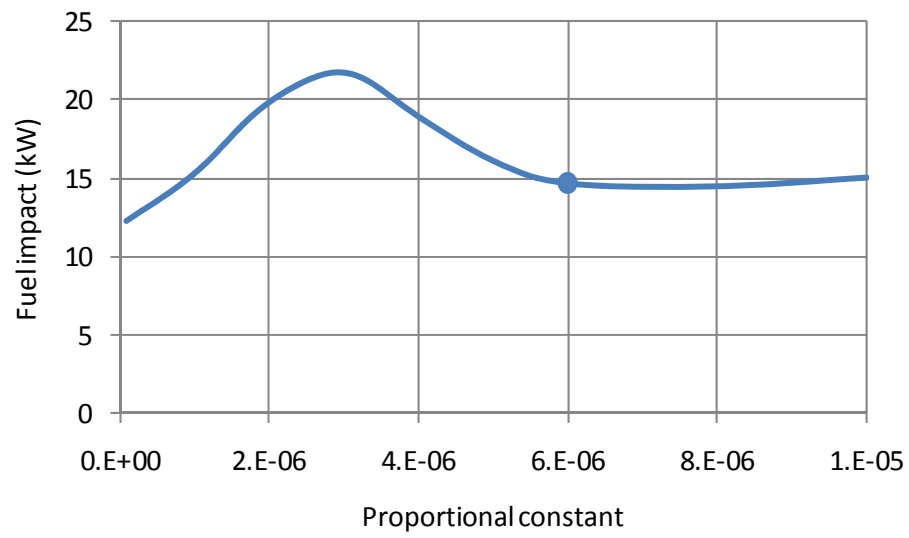


Figure 7. Effect of the proportional constant on the fuel impact

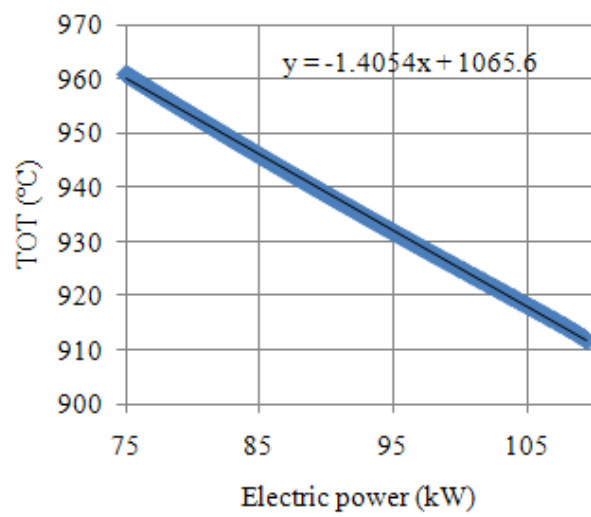


Figure 8. Turbine outlet temperature as the function of the electric load

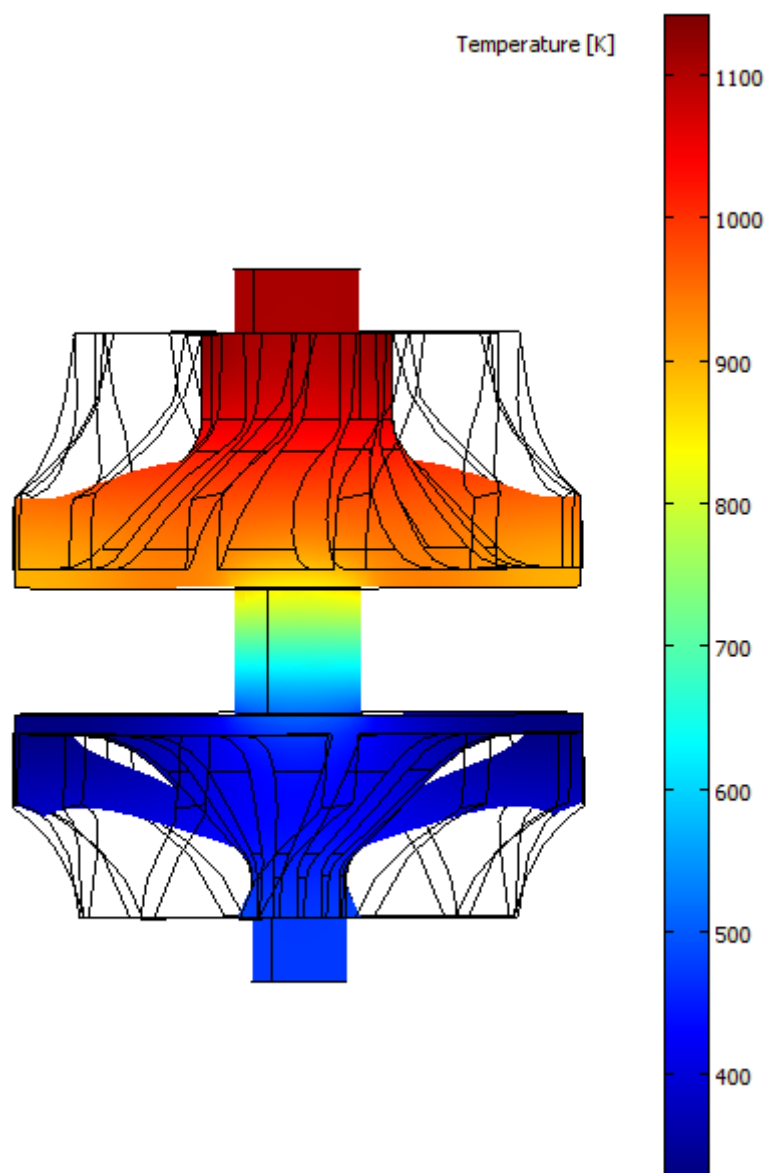


Figure 9. Temperature distribution in the turbine

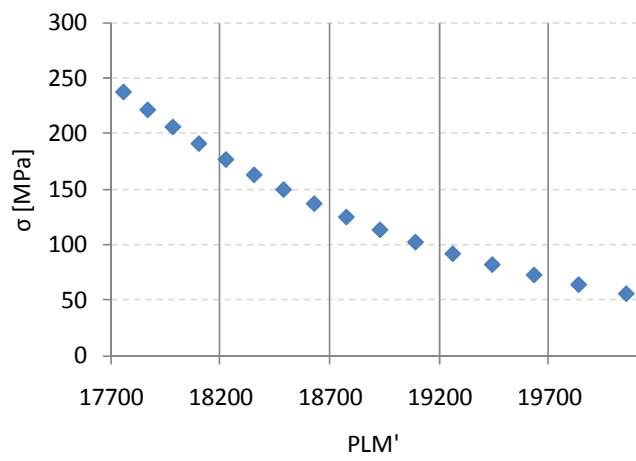


Figure 10. Larson-Miller curve

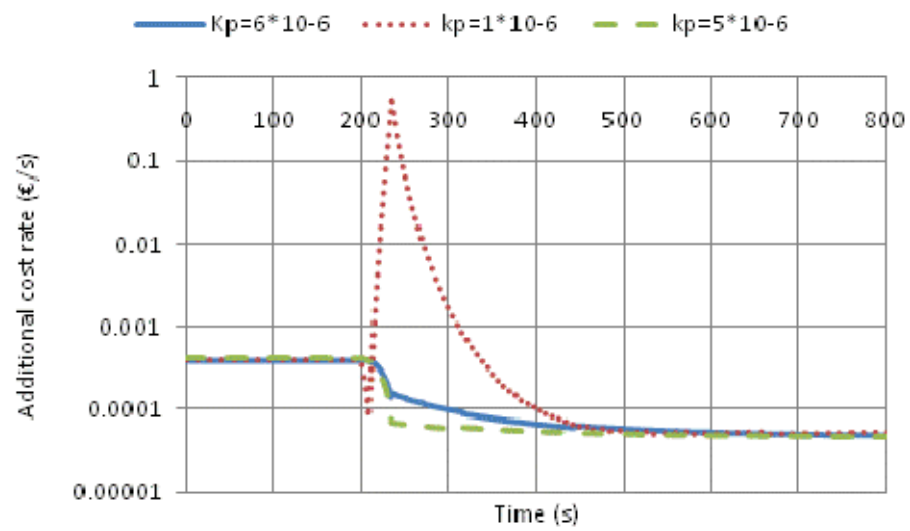


Figure 11. Additional costs corresponding to the first control strategy

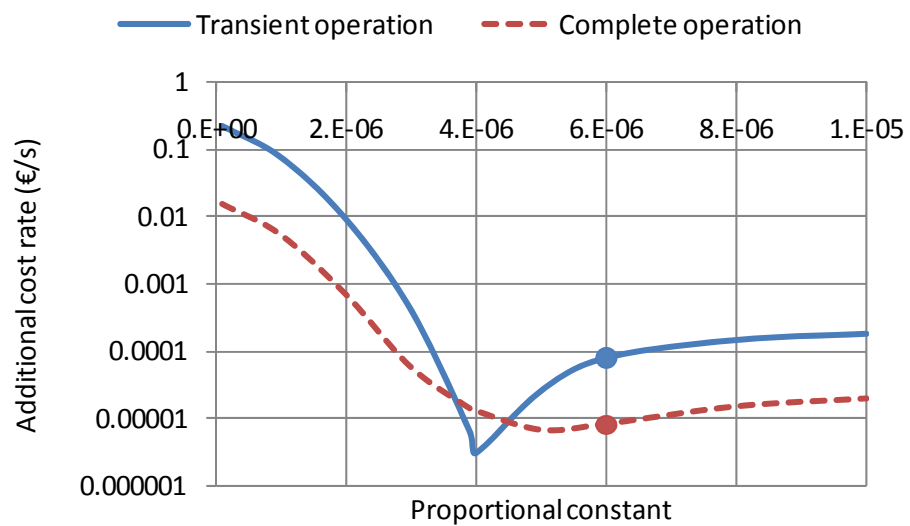


Figure 12. Additional cost rate in the transient operation

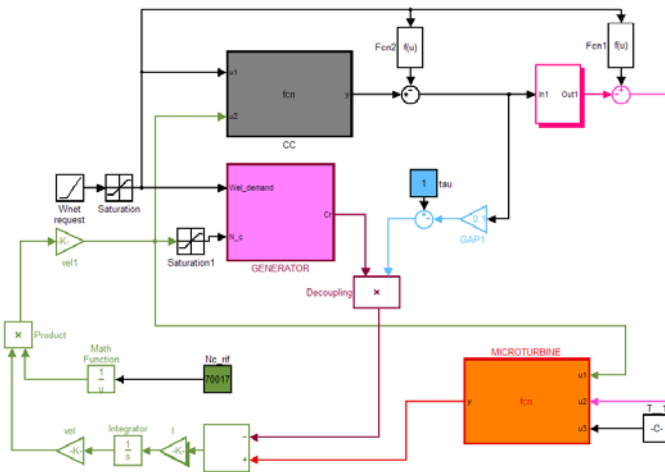


Figure 13. Scheme of the last control strategy



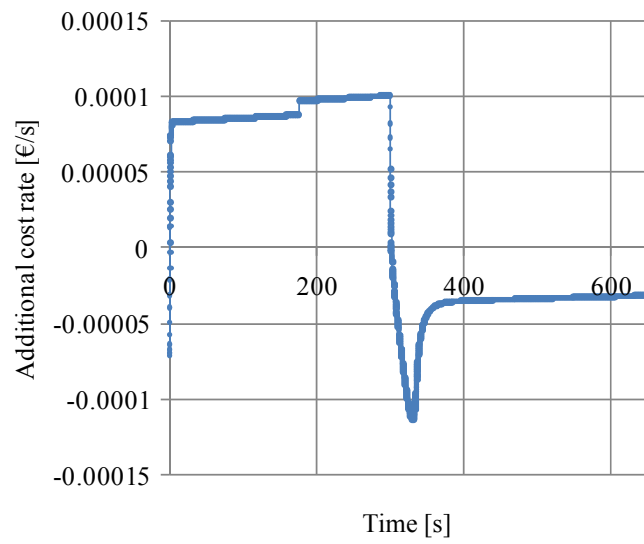


Figure 14. Additional costs corresponding to the second control strategy

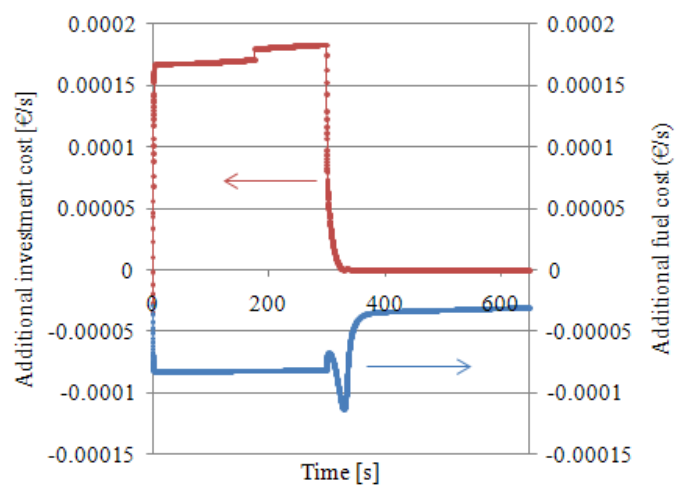


Figure 15. Contributions to the additional costs

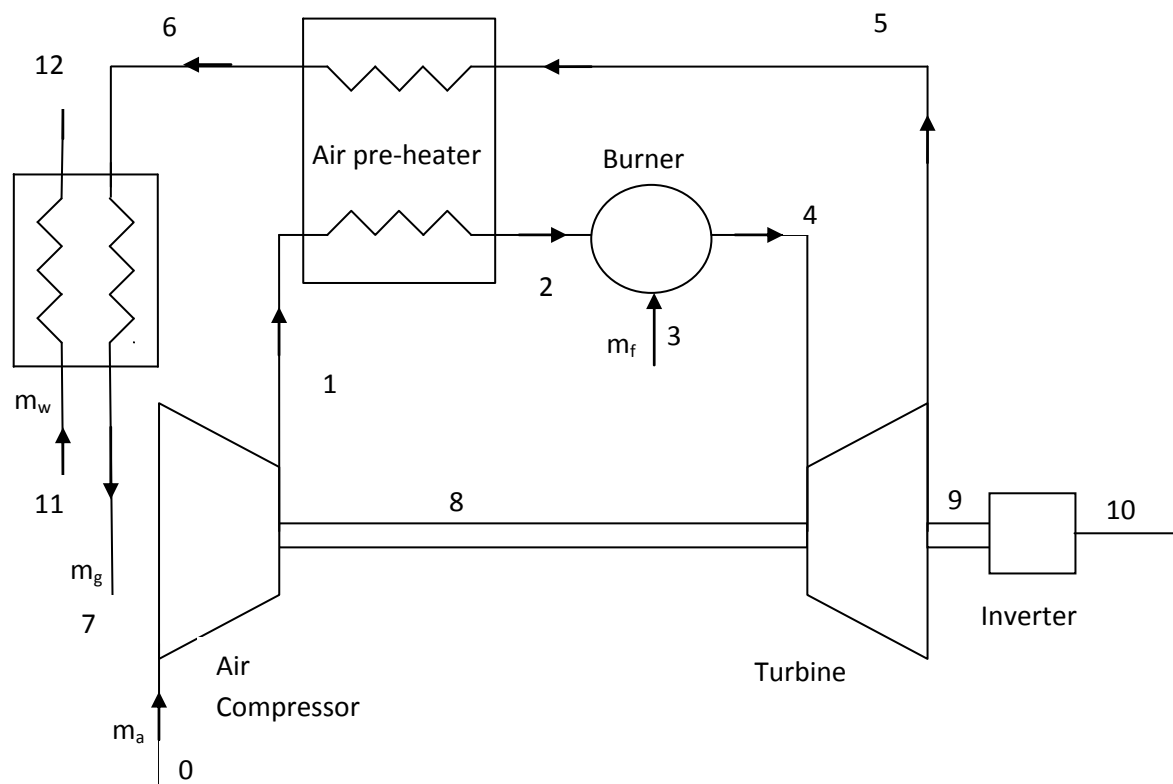


Fig. A1. Physical structure of the microturbine

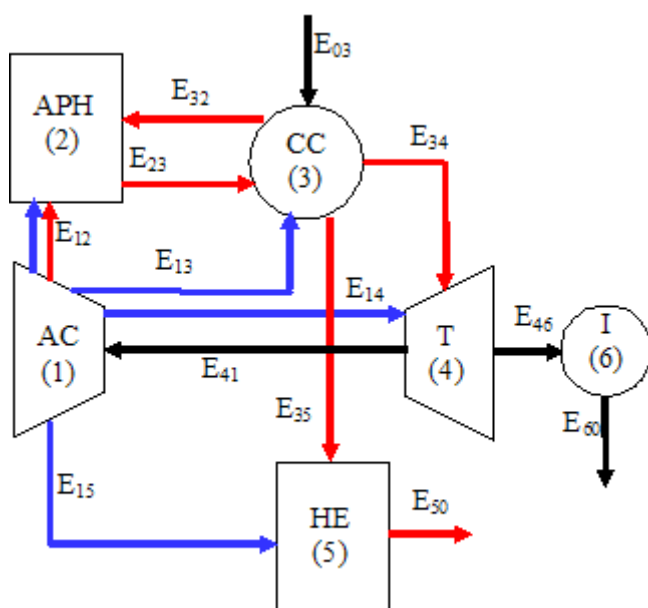


Fig. A2. Productive structure of the microturbine